Electronic Supplementary Material (ESI) for Chemical Communications.
This journal is © The Royal Society of Chemistry 2023

Supporting Information

Metal-mediated tunability of MOF-based optical modulators

Nikita K. Kulachenkov,[a] Bogdan Orlioglo,[b] Eugene S. Vasilyev,[c] Svyatoslav A. Povarov,[a] Alexander M. Agafontsev,[c,d] Semyon Bachinin,[a] Sergei Shipilovskikh,[a] Artem Lunev,[a] Denis G. Samsonenko,[e] Vladimir P. Fedin,[e] Konstantin A. Kovalenko,[e*] Valentin A. Milichko[a,f*]

[a] *School of Physics and Engineering, ITMO University, St. Petersburg, 197101, Russia*
[b] *Chemical Science Program, KAUST Catalysis Center, Division of Physical Science and Engineering, King Abdullah University of Science and Technology (KAUST), Thuwal, 23955-6900 Saudi Arabia*
[c] *Vorozhtsov Novosibirsk Institute of Organic Chemistry, Siberian Branch of Russian Academy of Sciences, 9 Acad. Lavrentiev Ave., 630090 Novosibirsk, Russia*
[d] *Novosibirsk State University, 2 Pirogova St., 630090 Novosibirsk, Russian Federation*
[e] *Nikolaev Institute of Inorganic Chemistry SB RAS, 3 Akad. Lavrentiev Ave., 630090 Novosibirsk, Russian Federation*
[f] *Institut Jean Lamour, Universit de Lorraine, UMR CNRS 7198, 54011 Nancy, France*

* Email: valentin.milichko@univ-lorraine.fr; k.a.kovalenko@niic.nsc.ru

Table of Contents

Experimental section

Methods

All organic solvents were used freshly distilled. Merck silica gel 60 (0.063–0.100 mm) was used for preparative column chromatography. Analytical TLC was carried out on a ready-to-use plates (SiO_2 on Al foil, visualization by spraying with a solution of $FeCl_3\cdot6H_2O$ or under UV light (254 nm). Other commercially available reagents were used without any purification.

The X-ray powder diffraction (PXRD) data were collected with Co-Kα radiation on a Shimadzu XRD 7000S powder diffractometer (step size of 0.03 deg/s; 2θ range from 3° to 35°). Elemental analysis (C, H, N) was performed on a Vario Micro Cube, Elementar. NMR spectra were recorded at 20–23 °C for solutions (C = 20–40 mg/mL) on a Avance 400 or Avance 300 spectrometer (Bruker Corporation, Billerica, MA, USA) locked to the deuterium resonance of the solvent. The chemical shifts were calculated relative to the solvent signals used as the internal standard: δC 76.90 ppm and δH 7.24 ppm for $CDCl_3$; δC 39.50 ppm and δH 2.50 ppm for DMSO-d6.The FT-IR spectra of the samples in KBr pellets were recorded on a Scimitar FTS 2000 or a Bruker TENSOR 27 Fourier-transform infrared spectrometers in the range of 4000–400 cm^{-1}. Optical rotation was measured on a PolAAr 3005 polarimeter (Optical Activity Ltd, Ramsey, Cambridgeshire, United Kingdom). Thermal gravimetric analysis were carried out using a NETZSCH TG 209 F1 Iris Thermo Microbalance at 25–600 °C in helium flow with heating rate of 10 $°C\cdot min^{-1}$. The precise molecular weights were determined by high-resolution mass spectrometry on a Bruker micrOTOF-Q (Atmospheric pressure electrospray ionization, API-ES) mass spectrometers.

Single crystal X-Ray analysis. Diffraction data for single crystals of compounds **1** and **2** were obtained at 130 K on an automated Agilent Xcalibur diffractometer equipped with an area CCD AtlasS2 detector (MoKα, graphite monochromator, ω-scans with a step of 0.25° for **1** and 0.50° for **2**). Integration, absorption correction, and determination of unit cell parameters were performed using the CrysAlisPro program package [1]. The structures were solved by the dual space algorithm (SHELXT [2]) and refined by the full-matrix least squares technique (SHELXL [3]) in the anisotropic approximation (except hydrogen atoms). Positions of hydrogen atoms of organic ligands were calculated geometrically and refined in the riding model. The crystallographic data and details of the structure refinements are summarized in Table S1. CCDC 2250659 (**1**) and 2250660 (**2**) contain the supplementary crystallographic data for this paper. These data can be obtained free of charge from The Cambridge Crystallographic Data Center at https://www.ccdc.cam.ac.uk/structures/.

Phase purity and thermal stability. The phase purity of the as-synthesized compounds was conirmed by the powder X-ray diffraction (PXRD) analysis, which is consistent with the simulated one from the SCXRD data (Figs. S3-S6). The obtained thermal stability is essential in further investigation of their functional optical properties. According to the thermogravimetric data in Figs. S9, S10, the compounds **1** and **2** demonstrate sufficiently high thermal stability, and coordinated water molecules are removed at temperatures above 180 °C and 200 °C, respectively. A further increase in temperature leads to a two-stage mass loss process, possibly corresponding to the degradation of the organic ligands.

Optical characterization. Optical transmission spectra for MOFs **1** and **2** settled on a glass substrate on air have been measured using a home-made confocal setup. The single crystals of each MOF have been irradiated by white light source (Avantes 360–2500 nm) via 10x/0.26NA objective in transmission geometry, while the transmission signal has been collected via 100x/0.9NA objective and then analysed by confocal spectrometer (HORIBA Labram, 150 g/mm diffraction grating and Andor water-cooling detector). The laser excitation of the single crystals has been implemented by fundamental (1047 nm) harmonic of Yb^{3+} femtosecond laser source (150 fs pulse duration, 80 MHz repetition rate, integral power up to 50 mW) for pumping, and supercontinuum laser (Fianium, 6 ps pulse duration, 60 MHz repetition rate, 10 nm line width and 0.1 mW integral power) for probing. Transmission spectroscopy with a time resolution has been implemented using a mechanical shutter modulating the pump intensity over time at a frequency of 1 to 10 Hz; while both white continuous wave light and the probing pulses (60 MHz repetition rate) have been considered as a continuous optical signal for the analysis by oscilloscope.

Synthesis of the ligand

The ligand, sodium (−)-(5R,7R)-2,6,6-trimethyl-5,6,7,8-tetrahydro-5,7-methanoquinoline-3-carboxylate (NaL), was synthesized according to general scheme S**1**. (−)-α-pinene was used as the starting chiral compound. Nopinane-annelated pyridine was prepared via pinocarvone oxime as described previously [4], [5]. The ester was then hydrolyzed to the carboxyl anion. The structure and purity of the ligand was confirmed by NMR spectroscopy.

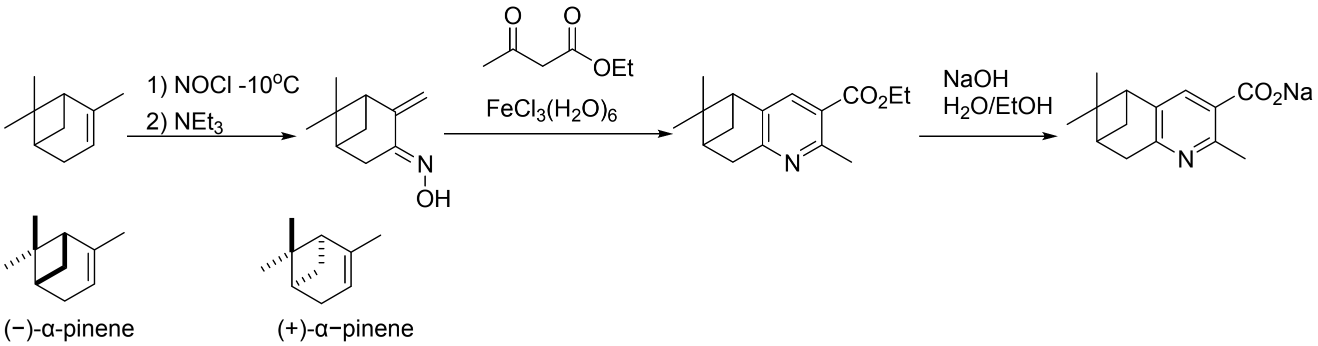

Scheme S1. General scheme of the ligands synthesis.

Ethyl (5R,7R)-2,6,6-trimethyl-5,6,7,8-tetrahydro-5,7-methanoquinoline-3-carboxylate

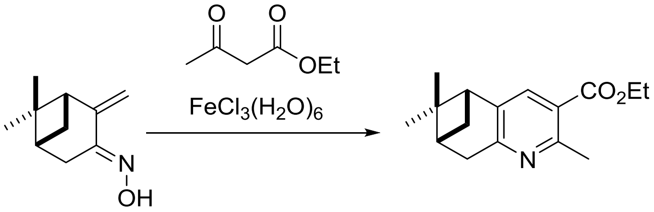

Scheme S2. Condensation of pinocarvone oxime with ethyl acetoacetate results in nopinane-annelated pyridine ester.

A mixture of (+)-pinocarvone oxime (1.65 g, 10 mmol), $FeCl_3 \cdot 6H_2O$ (0.54 g, 2 mmol) and ethyl acetoacetate (1.43 g, 11 mmol) was placed into a hot bath (130 °C). After stirring for 120 min at 130 °C, the mixture was cooled down to room temperature and diluted with EtOH (15 ml). Tartaric acid (3 g) was added to the solution, the resulting solution was treated with aqueous ammonia to pH > 9 and extracted with ethyl acetate (4 × 100 ml). The combined EtOAc extract was dried over

Na_2SO_4, filtered and concentrated under reduced pressure to leave the crude product which was purified by column chromatography (SiO_2, petroleum ether – EtOAc, 10:1 → 8:2, v/v) to afford pure compound. Yield: 0.82 g, 32%.

Sodium (5R,7R)-2,6,6-trimethyl-5,6,7,8-tetrahydro-5,7-methanoquinoline-3-carboxylate

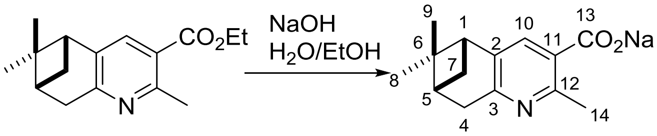

Scheme S3. Hydrolysis of the ester.

Sodium (0.370 g, 16.1 mmol) was dissolved in ethanol (20 mL), and water (25 mL) was added. The obtained sodium hydroxide solution was added to the solution of nopinane-annelated pyridine (4.18 g, 16.1 mmol) in ethanol (25 mL). The mixture was stirred at room temperature for 12 h while the reaction progress was controlled by TLC. The mixture was then diluted with water (150 mL) and extracted with diethyl ether (50 mL), the water layer was separated and concentrated under reduced pressure (rotary evaporator followed by a vacuum system). Yield: 3.99 g, 98%.

Yellowish crystals; $[\alpha]\frac{25}{D}$ −26 (c 0.957,CH_3OH); m.p. 318–319 °C; ^1H NMR (300 MHz, DMSO-d_6:D_2O=1:1): δ = 0.46 (*s*, 3H, H8), 1.02 (*d*, 1H, *J* = 9.8Hz, *pro-R*-H7), 1.26 (s, 3H, H9), 2.22 (*m,*1H, H5), 2.40 (*s*, 1H, H14), 2.58(*ddd,* 1H, *J* = 9.5, 5.8, 5.8Hz, *pro-S*-H7), 2.68 (*dd*, 1H, *J* = 5.8, 5.8Hz, H1), 2.85 (*d*, 1H, *J* = 2.0Hz, H4), 7.25 (*s*, 1H, H10);^{13}CNMR (125MHz, DMSO-d_6:D_2O=1-1): δ =22.18 (C8), 23.21 (C14), 26.77 (C9), 32.92 (C7), 36.59 (C4), 40.17 (C6), 40.85 (C5), 46.48 (1), 133.40 (C11), 134.58 (C10), 140.54 (C2), 152.74 (C3),156.65 (C2),175.76 (C13);

IR (1:150 w/w in KBr, $\nu_{max/}cm^{-1}$): 1576 (very strong) (-CO_2^-), 1412 (strong)(-CO_2^-).

HRMS (API-ES) calcd for $C_{14}H_{16}NO_2^-$: 230.118 $[M–H]^-$ found: 230.120; calcd for $(C_{14}H_{16}NO_2)_2Na^-$: 483.227 $[(M–H)_2Na]^-$ found: 483.227.

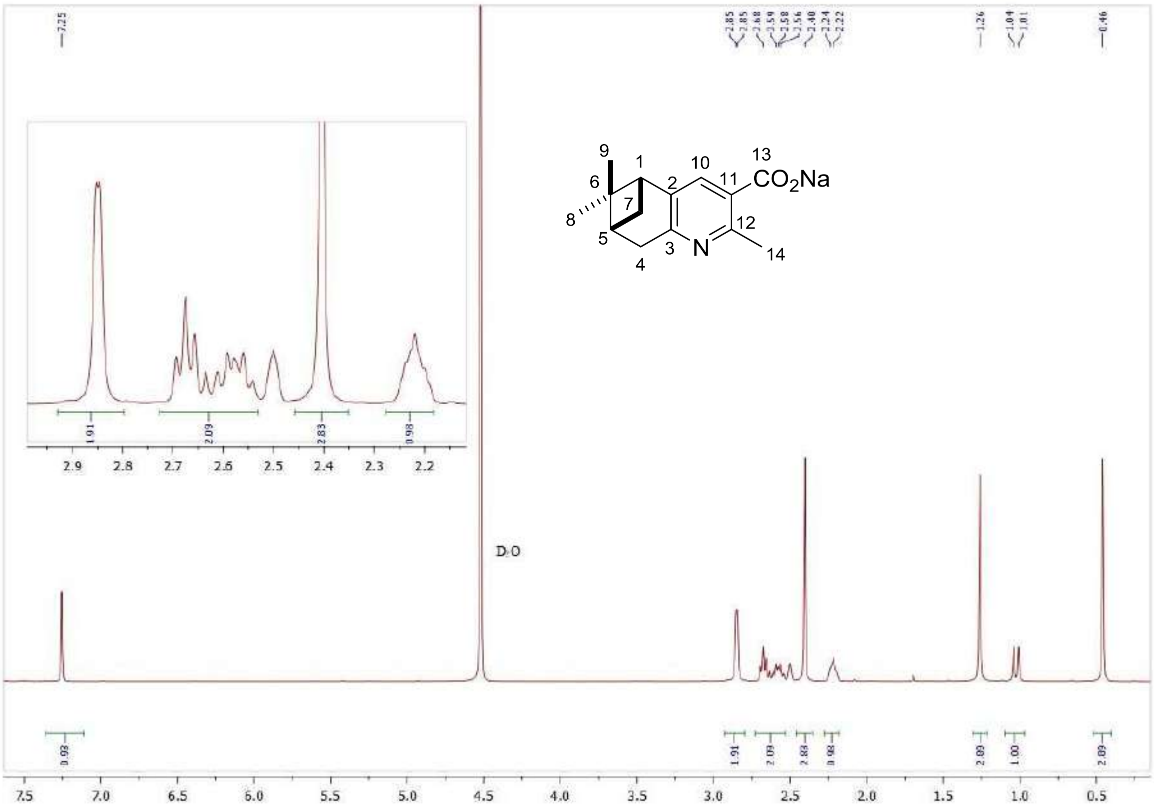

Fig. S1. ^{1}H NMR spectra (300 MHz, DMSO-d_6:D_2O=1:1) of sodium (5R,7R)-2,6,6-trimethyl-5,6,7,8-tetrahydro-5,7-methanoquinoline-3-carboxylate.

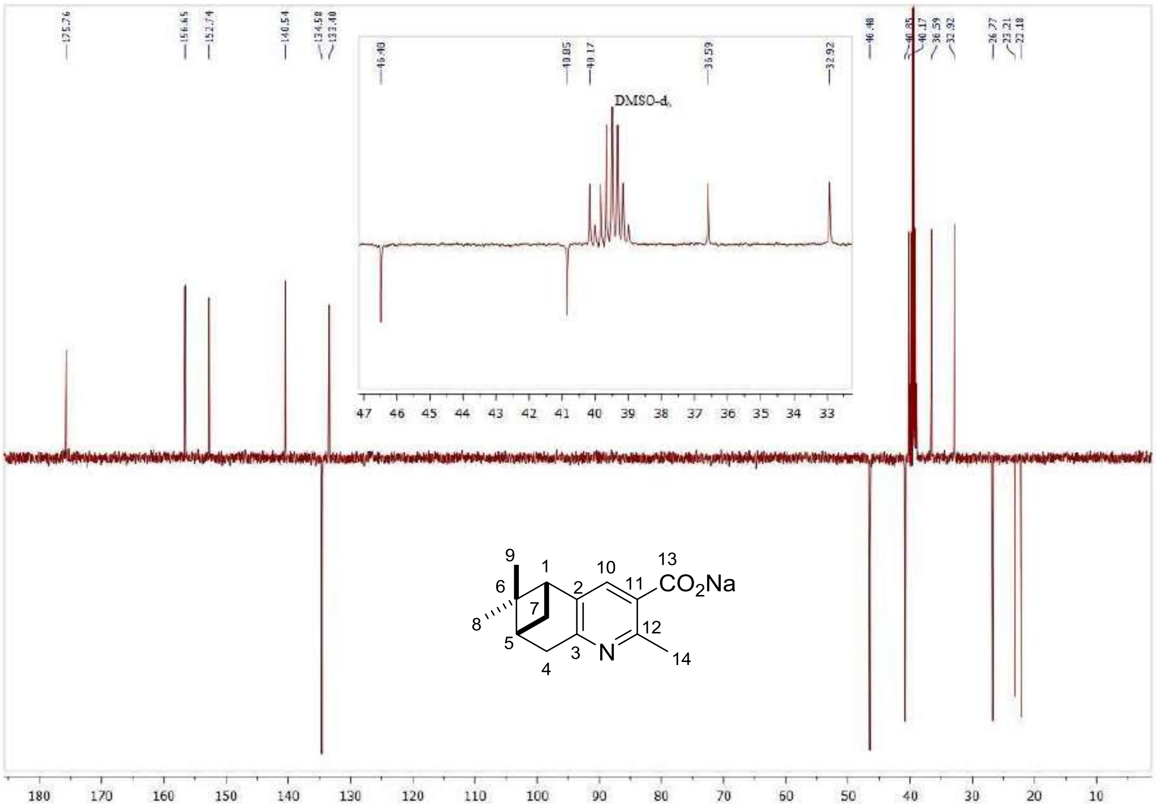

Fig. S2. ^{13}C J-modulation with BB-decoupling at ^{1}H (C,CH_2 - positive, CH,CH_3– negative NMR spectra (125 MHz, DMSO-d_6:D_2O=1:1) of sodium (5R,7R)-2,6,6-trimethyl-5,6,7,8-tetrahydro-5,7-methanoquinoline-3-carboxylate.

Synthesis of MOFs

Synthesis of [Co(bpe)(H$_2$O)L$_2$] (1)

A solution of $Co(ClO_4)_2 \cdot 6H_2O$ (7.2 mg, 0.02 mmol), NaL (10 mg, 0.04 mmol) and 1,2-di(4-pyridyl)ethylene (bpe) (3.6 mg, 0.02 mmol) in 8 mL mixture of equil volumes of EtOH and H_2O was heated at 100°C using sand bath in screw-caped glass vial with fine hole in order to allow solvent to evaporate slowly. After 2 days heating, only half of the solvent evaporated. Red needle-shaped crystals of **2** suitable for X-ray single crystal analysis were obtained and washed with H_2O and EtOH to remove brown amorphous residue. Yield: 5.8 mg (40% based on Co). *Anal.* Calc. for $C_{40}H_{44}CoN_4O_5$ (%): C, 66.8; H, 6.2; N, 7.8. Found: C, 66.5; H, 5.9; N, 7.6.

FT-IR (KBr pellets, ω/cm^{-1}): 553 (m), 663 (w), 719 (w), 767 (m), 808 (m), 1076 (m), 1205 (m), 1402 (s), 1477 (s), 1539 (m), 1606 (s), 2920 (s), 2968 (m), 3045 (m).

Synthesis of [Ni(bpe)(H$_2$O)L$_2$] (2)

A solution of $Ni(NO_3)_2 \cdot 6H_2O$ (5.7 mg, 0.02 mmol), NaL (10 mg, 0.04 mmol) and 1,2-di(4-pyridyl)ethylene (bpe) (3.6 mg, 0.02 mmol) dissolved in mixture of 1 mL of water and 1 mL of EtOH was heated in closed vial at 90 °C for 1 day using a sand bath. Green block crystals of **1** suitable for X-ray single crystal analysis were obtained and collected, washed with H_2O and EtOH to remove light-yellow amorphous residue. Yield: 5.8 mg (40% based on Ni). *Anal.* Calc. for $C_{40}H_{44}N_4NiO_5$ (%): C, 66.8; H, 6.2; N, 7.9. Found: C, 66.4; H, 6.3; N, 8.0.

FT-IR (KBr pellets, ω/cm^{-1}): 553 (s), 769 (m), 810 (s), 983 (m), 1020 (m), 1076 (w), 1207 (m), 1400 (s), 1479 (s), 1531 (s), 1608 (s), 2920 (s), 3062 (s).

Table S1. Crystal data and structure refinement for MOF **1**, and MOF **2**.

Parameter	**1**	**2**
Empirical formula	$C_{40}H_{44}CoN_4O_5$	$C_{40}H_{44}N_4NiO_5$
M, g/mol	719.72	719.50
Crystal system	Monoclinic	Monoclinic
Space group	$P2_1$	$P2_1$
a, Å	13.6588(3)	13.5294(6)
b, Å	9.30808(16)	9.2669(3)
c, Å	28.8554(6)	28.7704(12)
β, deg.	95.8388(16)	95.680(4)
V, Å^3	3649.56(13)	3589.4(2)
Z	4	4
D(calc.), g/cm^3	1.310	1.331
μ, mm^{-1}	0.519	0.590
F(000)	1516	1520
Crystal size, mm	0.34 × 0.27 × 0.10	0.24 × 0.14 × 0.07
θ range for data collection, deg.	2.13–25.68	2.31–25.35
Index range	$-16 \le h \le 16$, $-11 \le k \le 11$, $-35 \le l \le 24$	$-12 \le h \le 16$, $-11 \le k \le 11$, $-34 \le l \le 34$
Reflections collected / independent	33497 / 18794	27237 / 13131
R_{int}	0.0337	0.0309
Reflections with $I > 2\sigma(I)$	16747	11880
Goodness-of-fit on F^2	0.990	1.115
Absolute structure parameter	0.048(5)	0.048(16)
Final R indices [$I > 2\sigma(I)$]	$R_1 = 0.0325$, $wR_2 = 0.0736$	$R_1 = 0.0474$, $wR_2 = 0.0973$
R indices (all data)	$R_1 = 0.0384$, $wR_2 = 0.0751$	$R_1 = 0.0550$, $wR_2 = 0.0996$
Largest diff. peak / hole, e/Å^3	0.349 / −0.255	0.719 / −0.549

Physicochemical characterization of MOFs 1 and 2

The as-synthesised MOFs **1** and **2** are isomorphous and crystallize in the monoclinic non-centrosymmetric P21 chiral space group (Table S1). The asymmetric unit comprises two independent M^{2+} ions with a distorted octahedral geometry (Fig. 1a, S3-S4). Each metal ion is coordinated by two nitrogen atoms from two bridging bpe ligands in the *trans*-position to each other and four oxygen atoms, two of which are from the κ^2-coordinated carboxylic group of the L^- ligand, another one is from the κ^1-coordinated carboxylic group of the second L^- ligand, and the last one is from the water molecule. The geometry of coordinated bpe ligands permits the formation of two chains (Fig. 1b). The distance between two independent ions in the asymmetric unit is 8.136 Å. Moreover, there are hydrogen bonds between water molecules and the uncoordinated oxygen atom of the κ^1-coordinated carboxylic group with *d*(O–H···O) = 2.613–2.646 Å as well as a second one with the pyridine nitrogen atom of the κ^1-coordinated L^- ligand of the neighbour chain with *d*(O–H···N) = 2.805–2.835 Å. Short contacts, corresponding to weak interactions between neighbour chains, have also been detected between aromatic and aliphatic C–H and oxygen of the κ^2-coordinated carboxylic group with *d*(C···O) = 3.29–3.36 Å and between aliphatic CH_2-groups of the bicyclic fragment of the κ^1-coordinated L^- ligand and the pyridine nitrogen atom of the κ^2-coordinated L^- ligand with *d*(C···N) = 3.53–3.55 Å. The MOFs obtained have been thoroughly characterized using powder X-Ray diffraction (PXRD, Figs. S5–S7), FTIR (Fig. S8), TG (Fig. S9,S10) and elemental C, H, and N analysis (see details below).

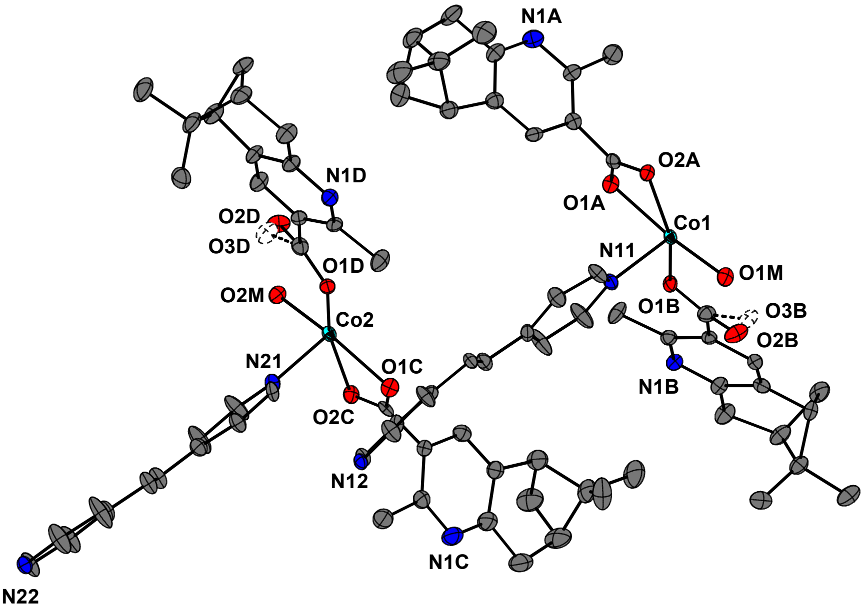

Fig. S3. Asymmetric unit of the structure **1** (H atoms are omitted). The second position of disordered atoms are shown with dashed lines.

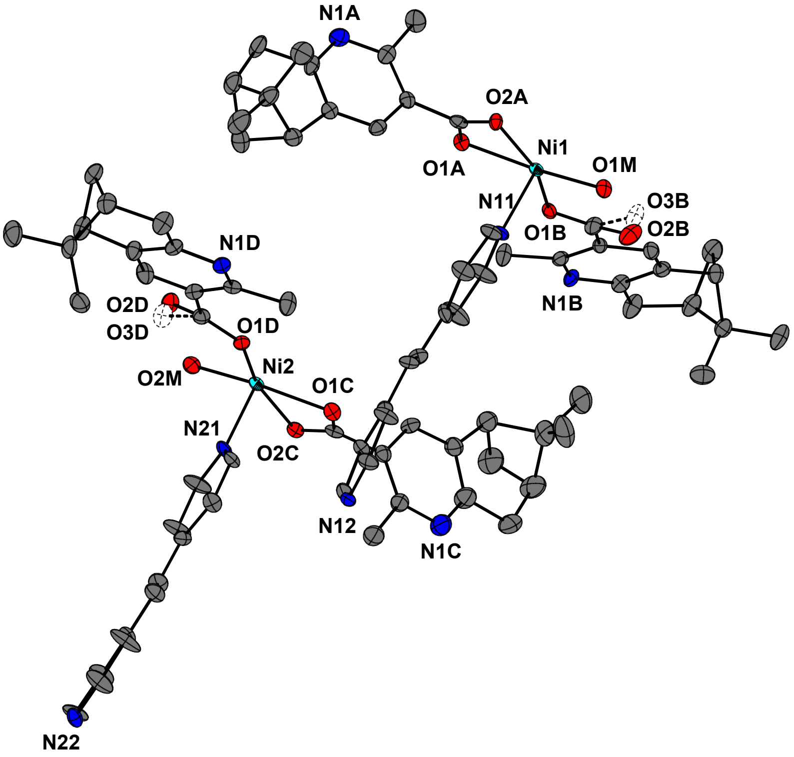

Fig. S4. Asymmetric unit of the structure **2** (H atoms are omitted). The second position of disordered atoms are shown with dashed lines.

PXRD of as synthesized MOFs

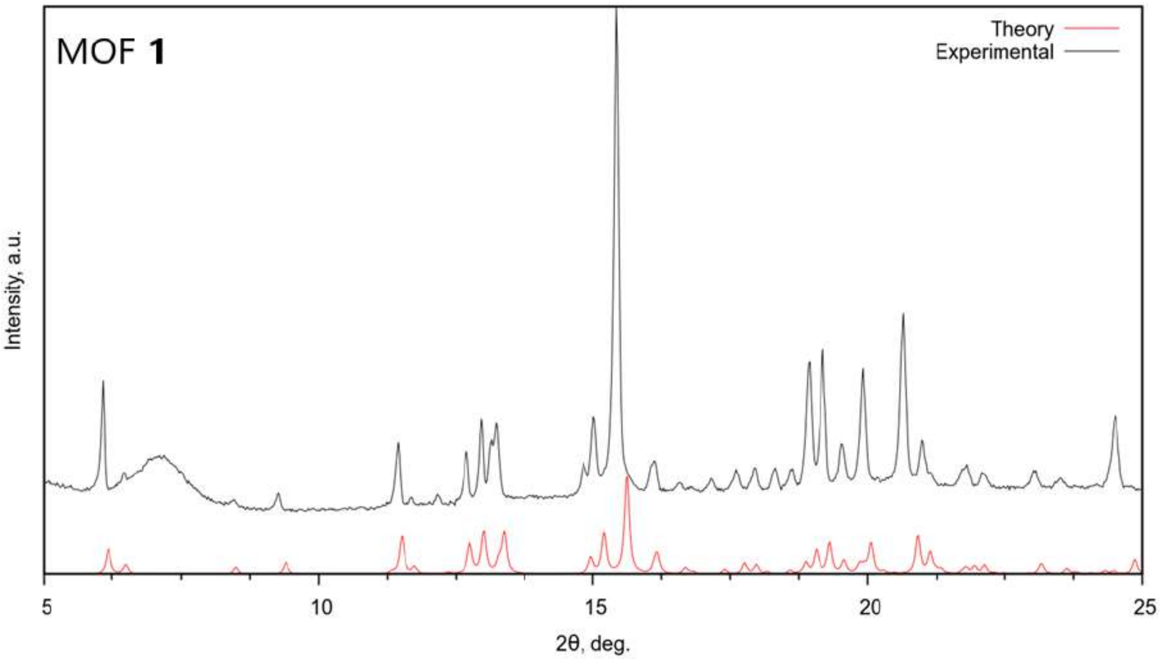

Fig. S5. PXRD pattern of MOF **1** compared with patterns simulated from the single-crystal data.

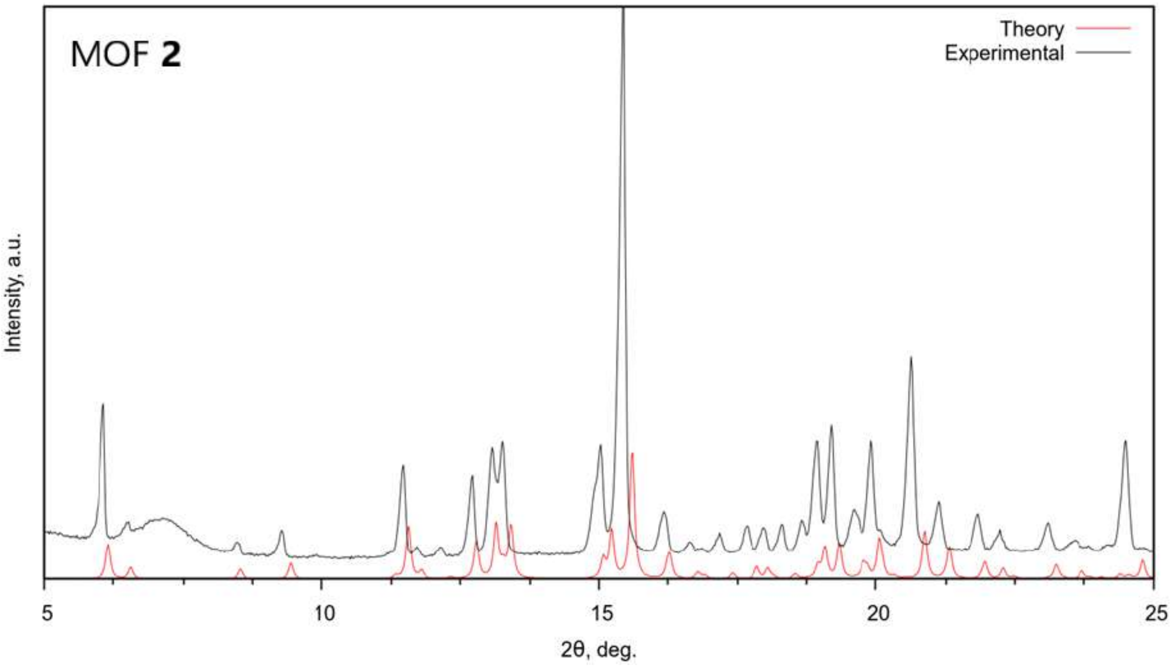

Fig. S6. PXRD pattern of MOF **2** compared with patterns simulated from the single-crystal data.

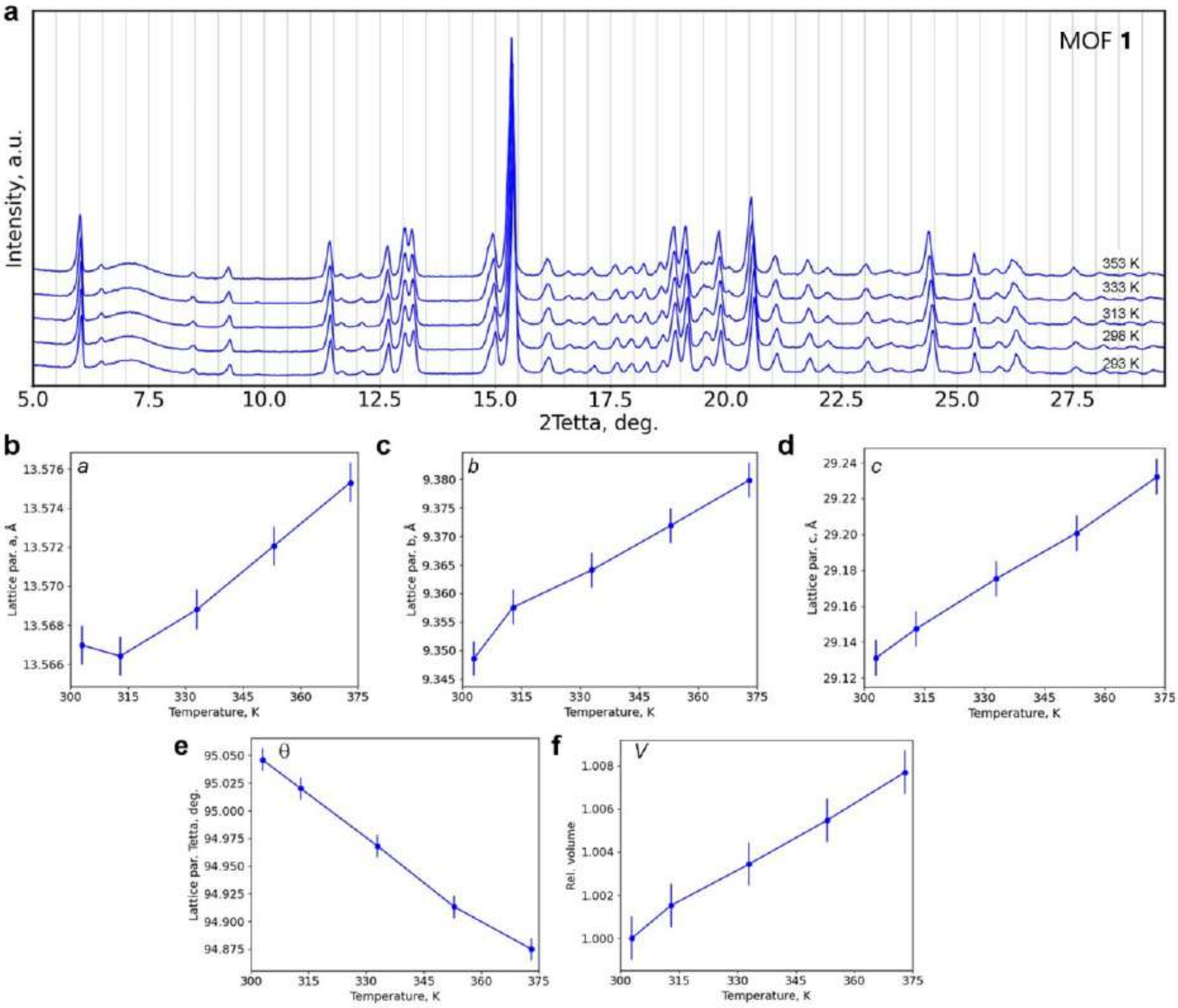

Fig. S7. (a) PXRD patterns for MOF **1** upon heating. (b–f) Dependence of crystal structure parameters of **1** on temperature.

FT-IR

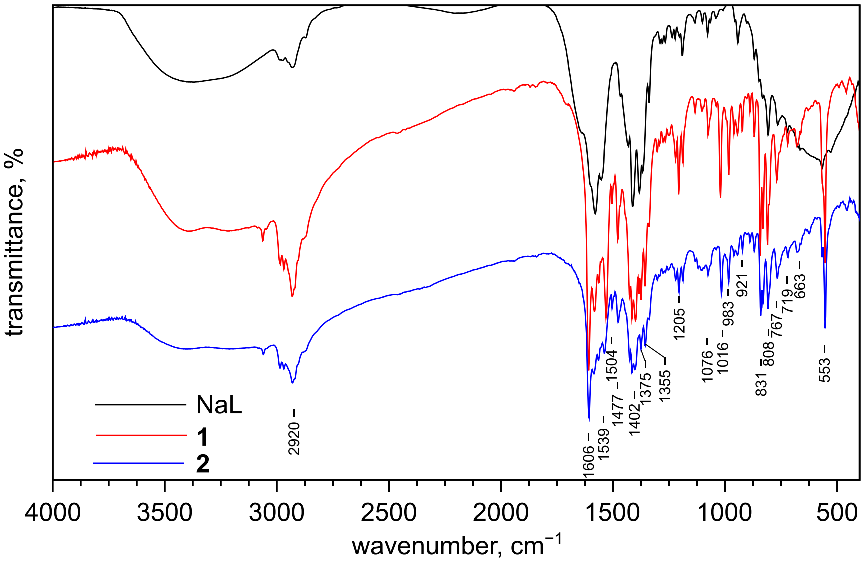

Fig. S8. FT-IR spectra of MOFs **1** and **2** in comparison with NaL.

TGA

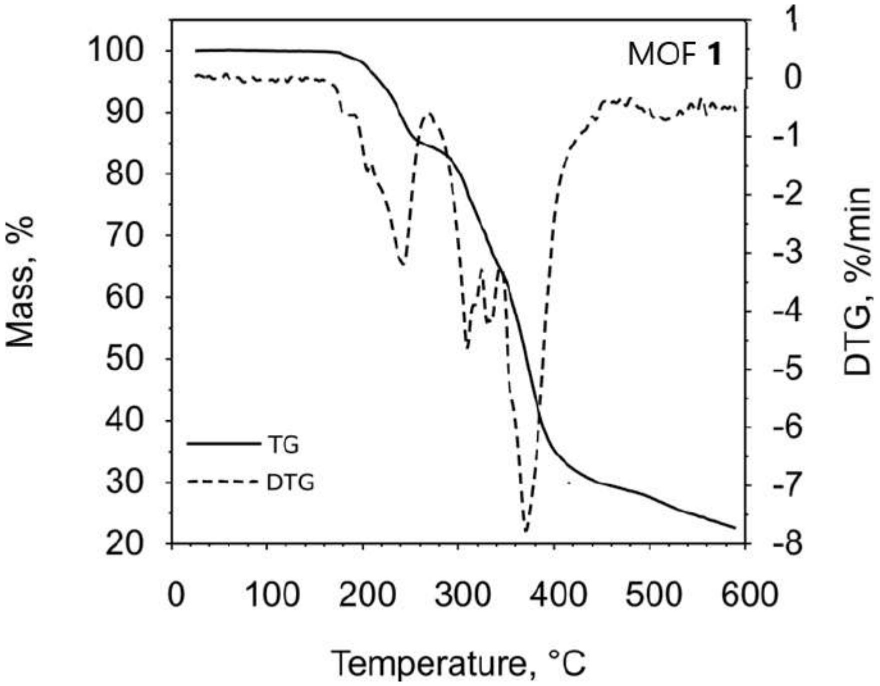

Fig. S9. TGA curves (solid lines) and DTG curves (dash lines) of MOF **1**.

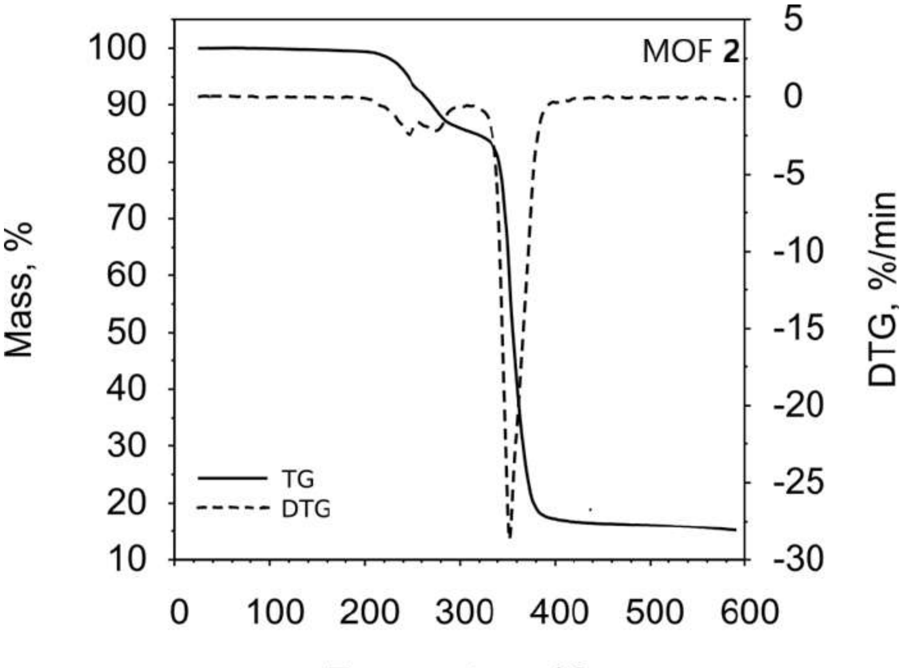

Fig. S10. TGA curves (solid lines) and DTG curves (dash lines) of MOF **2**.

Optical characterization of MOFs 1 and 2

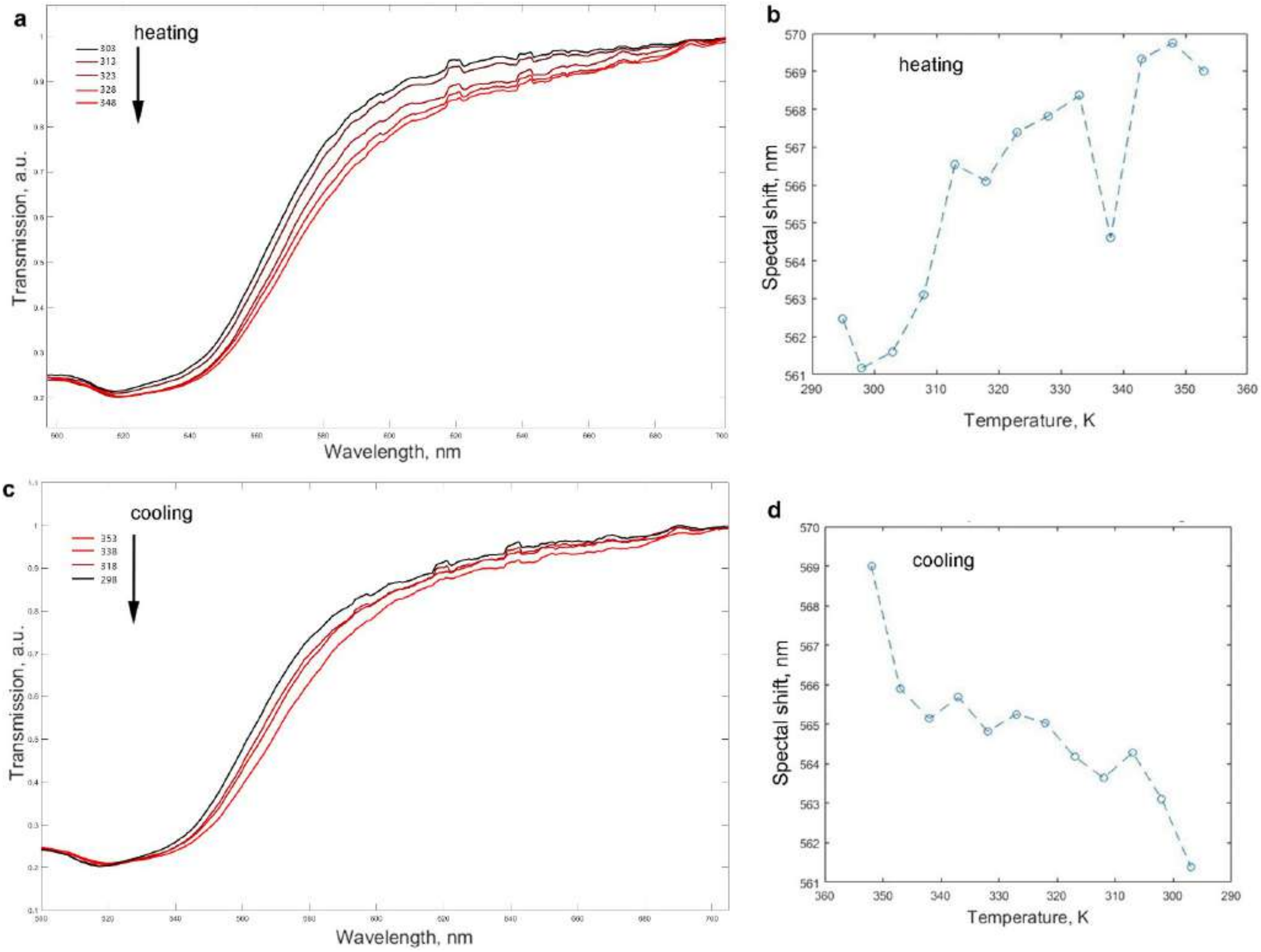

Fig. S11. Normalized optical transmission spectra for MOF **1** single crystal obtained upon heating and cooling on the Peltier stage.

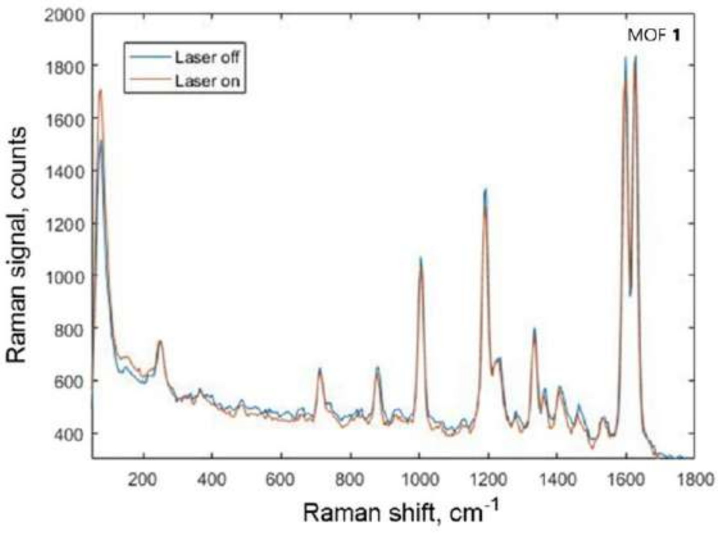

Fig. S12. Raman spectra for MOF **1** demonstrating the structural stability upon the action of 1047 nm laser pump (150 fs, 80 MHz repetition rate, and 40 mW integral power).

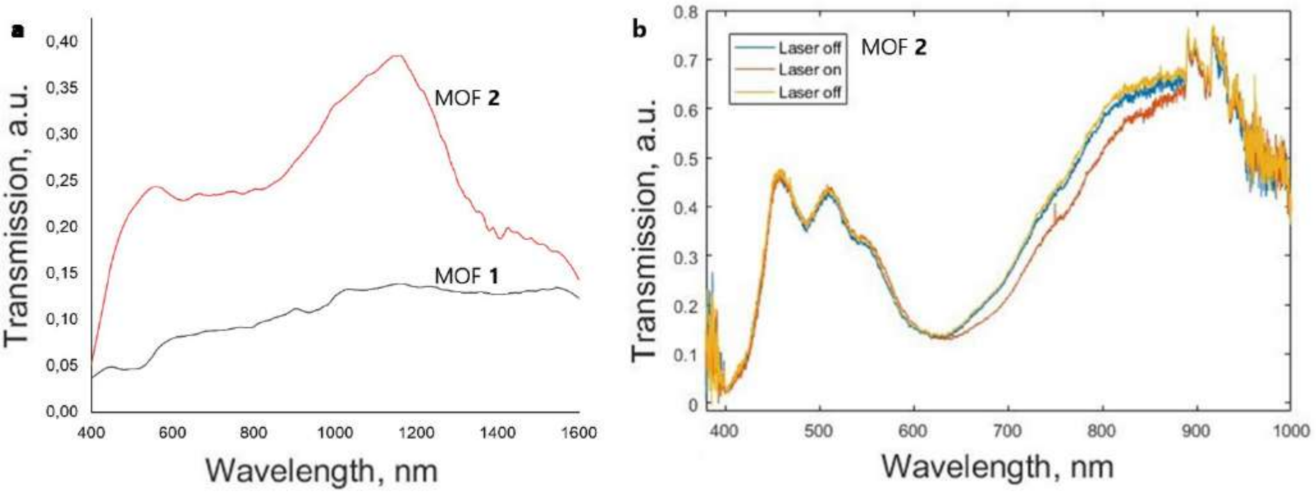

Fig. S13. (a) Optical transmission spectra of single crystal of MOF **1** and **2** (300 and 150 μm thick, respectively) in the initial state. (b) Optical transmission spectra of single crystal of MOF **2** (100 μm thick) before, during, and after the action of 1047 nm laser pump (40 mW integral power). The data allows one to estimate the absorption coefficient ($\alpha = 6.93 * 10^3\ m^{-1}$) at a wavelength of 1000 nm for the MOF **2**.

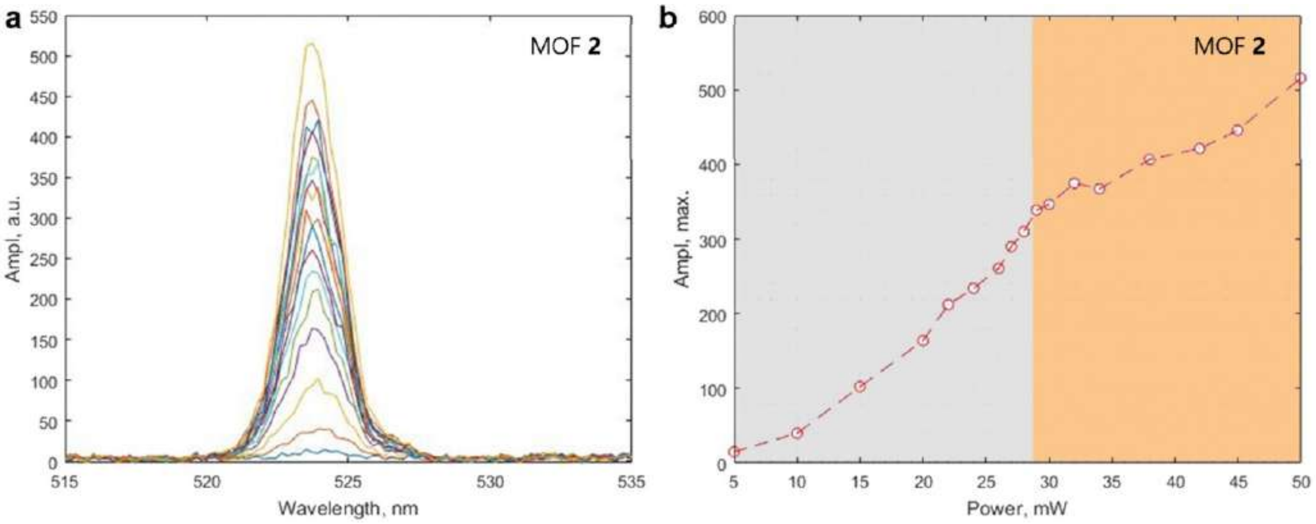

Fig. S14. Second harmonic generation of single crystal of MOF **2** (a) and the evolution of its intensity over the pumping laser power (b).

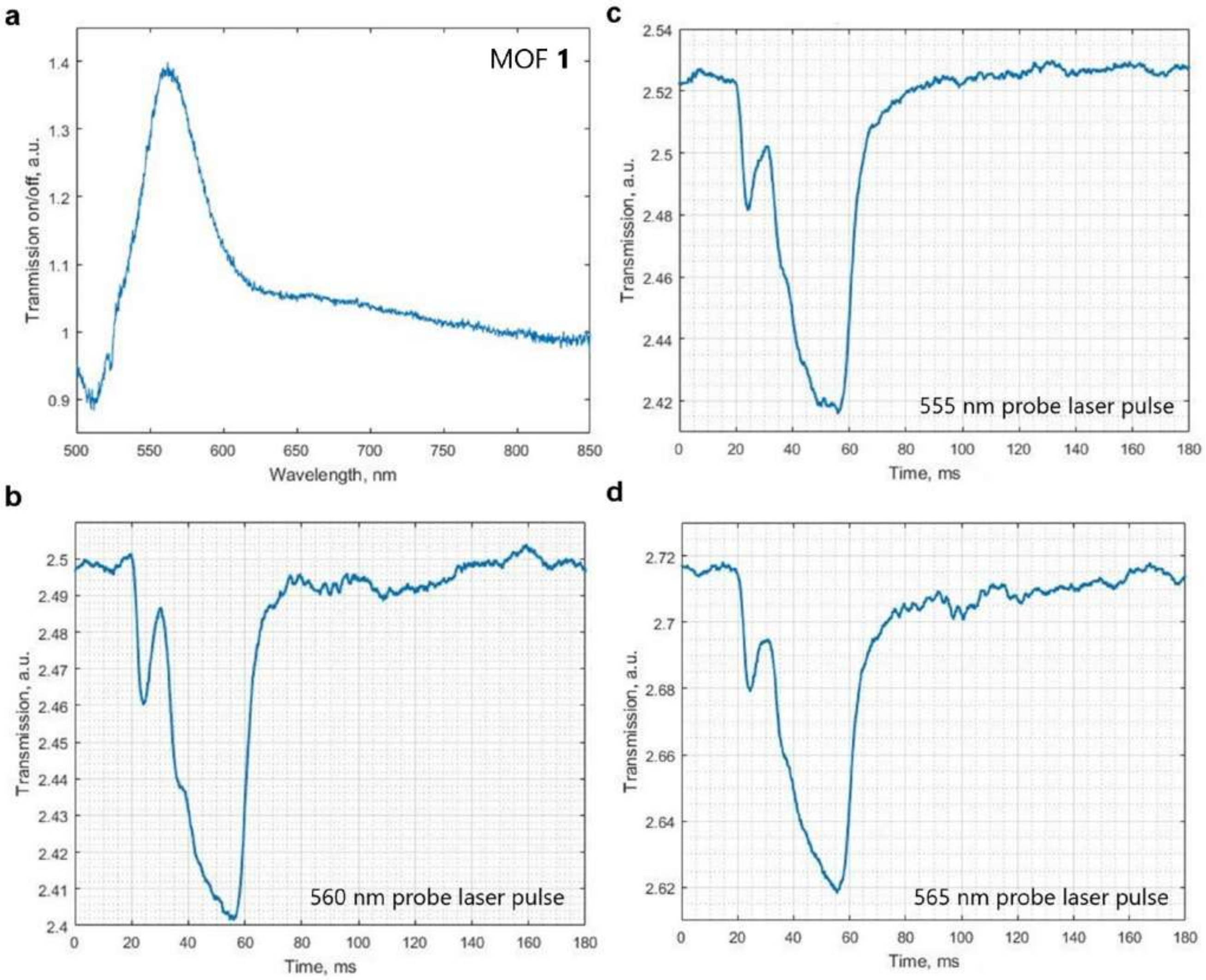

Fig. S15. (a) The on/off ratio of the optical transmission spectra in excited (on) and initial (off) states for MOF **1** with corresponding time evolution of the intensity of laser probes (555, 560, and 565 nm), passing through the MOF **1**, upon the action of a 1047 nm laser pump (b–d). The normalized signals in (b–d) are expressed as ratio of the laser probe intensity before and during the laser pump.

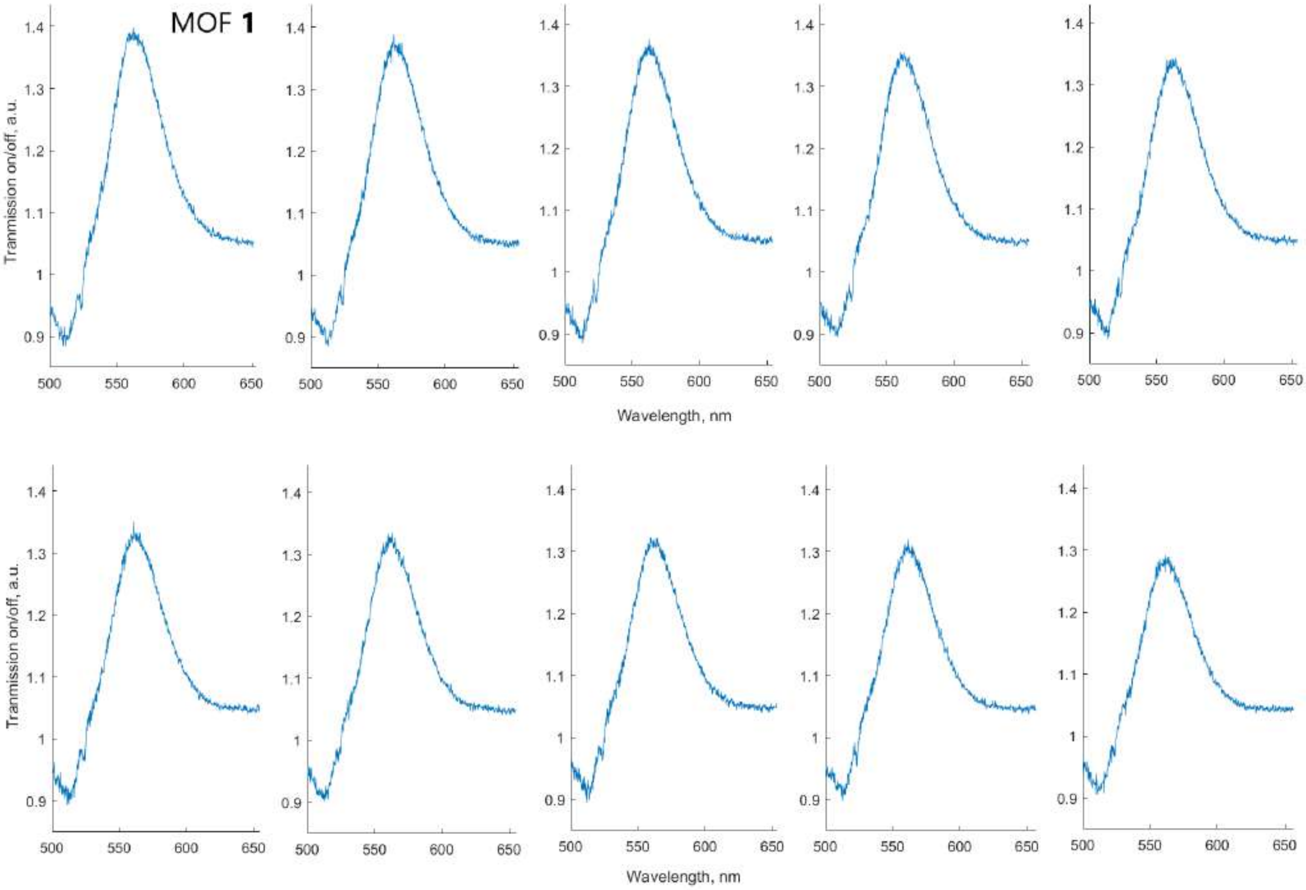

Fig. S16. Statistical analysis of the on/off ratio of the optical transmission spectra in excited (on) and initial (off) states for 10 different crystals of MOF **1**.

References

[1] CrysAlisPro Software system, version 1.171.38.46. Rigaku Oxford Diffraction, Rigaku Corporation, Wrocław, Poland, 2015.

[2] Sheldrick GM. *SHELXT* – Integrated space-group and crystal-structure determination. Acta Crystallogr. Sect. A 2015, 71, 3–8.

[3] Sheldrick GM. Crystal structure refinement with *SHELXL*. Acta Crystallogr. Sect. C 2015, 71, 3–8.

[4] Chibiryaev AM, De Kimpe N, Tkachev AV. Michael addition of ethyl acetoacetate to α,β-unsaturated oximes in the presence of FeCl3: a novel synthetic route to substituted nicotinic acid derivatives. Tetrahedron Letters 2000, 41, 8011–8013.

[5] Tkachev AV. Nitrosochlorination of terpenic compounds. Mendeleev Chem. J. 1998, 42.